Olfactory object recognition based on fine-scale stimulus timing in *Drosophila*

Aarti Sehdev[1†], Yunusa G. Mohammed[1†], Tilman Triphan[2], Paul Szyszka[1*]

[1] University of Konstanz, Department of Biology, Neurobiology, Konstanz, 78457, Germany

[2] University of Leipzig, Institute of Biology, Department of Genetics, Leipzig, 04103, Germany

[†] These authors contributed equally to this work.

[*] Corresponding author. Email: paul@szyszkalab.com

Abstract

Odorants of behaviorally relevant objects (e.g., food sources) intermingle with those from other sources. Therefore, to sniff out whether an odor source is good or bad – without actually visiting it – animals first need to segregate the odorants from different sources. To do so, animals could use temporal cues, since odorants from one source exhibit correlated fluctuations, while odorants from different sources are less correlated. However, it remains unclear whether animals can rely solely on temporal cues for odor source segregation. Here we show that flies can use temporal differences in odorant arrival down to 5 milliseconds to segregate mixtures of attractive and aversive odorants, and odor source segregation works for odorants with innate, as well as learned valences. Thus, the insect olfactory system can use stimulus timing for olfactory object segregation, similar as mammalian auditory or visual systems use stimulus timing for concurrent sound segregation and figure-ground segregation.

Introduction

A natural scene is comprised of primary stimulus features, such as the spectral reflectance, intensity and movement of objects. In addition, it consists higher-order stimulus features that reflect the spatial and temporal coherence of those stimuli that belong to the same object (e.g., the correlated movements of a person's body parts that allow us to segregate the person from the crowd). The mechanisms of how sensory systems use higher-order stimulus features for object recognition have been intensively studied in vision (*1*) and audition (*2*), but not in olfaction. Olfaction research has mainly focused on primary stimulus features, such as chemical identity, concentration and dynamics of olfactory stimuli (*3*, *4*), yet it is still unknown how the olfactory system processes higher-order stimulus features that underlie olfactory object recognition.

Olfactory object recognition involves recognizing whether intermingling odorants originate from the same or different sources (*5*). The capability to segregate odor sources is behaviorally relevant. For example, it allows animals to ignore spoiled food (food and detrimental odorants originate from the same source) and to find good food in a patch of spoiled food (food and detrimental odorants originate from different sources) without actually visiting the source.

Odor source segregation can be achieved from afar by analyzing the spatial distribution of odorants in a plume. This is because the different odorants from a single source form plumes with stable odorant concentration proportions (homogeneous plumes), while odorants from different sources form plumes with variable odorant concentration proportions (heterogeneous plumes) (*5*, *6*). Correspondingly, plume heterogeneity enables animals to segregate odor sources (slugs: (*7*), insects: (*8–11*), crabs: (*12*)). But how do they do it? An animal could use spatial sampling to detect the spatial heterogeneity of odorant concentrations by comparing odorant inputs along or between their olfactory organs. This strategy is

plausible for animals with long olfactory tentacles (slugs), antennae (insects) and antennules (crabs), but this strategy might not work for animals with small and narrow olfactory organs, such as fruit flies, because they lack spatial resolution. Alternatively, animals could use temporal sampling to detect timing differences in odorant arrival for odor source segregation, as the homogenous odorant plumes from a single source exhibit more correlated fluctuations than the heterogeneous odorant plumes from different sources (*5*, *6*). The latter strategy might be the only one available for small animals, such as fruit flies. This affords the possibility of using the fruit fly to investigate selectively how temporal cues can be used for odor-object segregation.

The neural mechanism by which a heterogeneous odor plume is segmented into its constituent odor objects is unknown. Determining the causal relationship between behavioral odor source segregation and neural activity requires a genetically tractable organism that allows manipulating neural activity in identified neurons. As this is possible in the fruit fly *Drosophila melanogaster*, we here studied flies' capability to use temporal stimulus cues for odor source segregation and demonstrate that flies can use few milliseconds short differences in odorant arrival (referred to as onset asynchrony) to segregate odorants with opposing innate or learned valences. The flies' rapid olfactory processing observed here lays the foundations for causal studies on the mechanisms of olfactory object recognition and implies a rapid and temporally precise mechanism for the encoding of olfactory objects.

Results

To ascertain whether flies can use stimulus onset asynchronies to segregate odorants in a plume, we used a free-flying behavioral paradigm in a wind tunnel (Fig. 1A and 1B) to test flies' preference to binary mixtures of attractive and aversive odorants with different onset asynchronies. We presented short pulses of single odorants or odorant pairs. To mimic homogeneous odorant plumes from one source we presented both odorants as a synchronous mixture (no onset delay between odorants), and to mimic heterogeneous odorant plumes from different sources we presented both odorants as asynchronous mixtures (with 5 to 33 millisecond delays between odorant onsets) (Fig. 1C). Note that all data shown in a given plot were collected in parallel to eliminate between-session variability. Accordingly, data points should be compared within plots but not between plots.

Tracking of temporally well-controlled odorant stimuli in the wind tunnel

We initially determined how reliable our stimulus delivery was over time by using a photoionization detector (PID) to record the stimulus dynamics of the different odorants used (Fig. 1D - 1I, S1A-C). The inlet of the PID was placed at the surface of the take-off platform (Fig. 1B). Each odorant was presented 50 times within its odorant pair 2-butanone (BN) and butanal (BA), BN and benzaldehyde (BZ), or 2,3-butanedione (BD) and ethyl acetate (EA). The onset times (time it took from valve opening to reach 5 % of the maximum PID signal) were temporally precise across trials, with standard deviations ranging between 6 ms (BN, BA) and 10 ms (BD, EA) (Fig. 1F, 1G and S1B).

The onset times were similar for all odorant pairs (BN/BA, BN: 744 ms ± 6 ms, BA: 745 ms ± 6 ms; BN/BZ, BN: 750 ms ± 7 ms, BZ: 756 ms ± 7 ms; BD/EA, BD: 691 ms ± 10 ms, EA: 691 ± 10 ms; mean ± SD). The rise times (time it took to reach from 5 % to 95 % of the maximum PID signal) were also similar for the odorant pair BN/BA (BN: 411 ± 10 ms, BA: 428 ± 12 ms; mean ± SD) and for the odorant pair BD/EA (BD: 428 ms ± 26 ms, EA: 440 ms ± 21 ms), but less similar for the odorant pair BN/BZ (BN: 400 ms ± 12 ms, BZ: 444 ms ± 9 ms) (Fig. 1H, 1I and S1C). The differences in stimulus dynamics could be explained by the difference in the molecular mass between odorants, as stimulus dynamics get slower with increasing molecular mass (in g/mol, BN: 72; BA: 72; BD: 86; EA: 88; BZ: 106) (*13*, *14*).

To visualize how flies explored space based on the odorant experience, we tracked their flights in 3D. For analysis, we projected the trajectories on a plane, and calculated the probability across flies to visit a

particular pixel (visit probability, Fig. 2A). When presented with an attractive odorant A flies were more likely to fly towards the target (which was either the actual odor source or a black platform near the odor source, see Materials and Methods), compared to the aversive odorant B. To assess approach to the target, we counted the number of flies which reached halfway between the center of the take-off platform and the target (3.1 cm (117 pixels) for WT 1 and 2.7 cm (71 pixels) for WT 2) and calculated the approach probability by dividing this number by the total number of flies. Flies flew closer towards the target when stimulated with an attractive odorant than with an aversive odorant or a control air stimulus (Air) ($p(A > B) \geq 0.999$ for BN/BZ in Fig. 1B; $p(A > B) = 0.962$, $p(A > Air) \geq 0.999$ for BN/BA/Air in Fig. 1C ; all statistical significances are given as Bayesian probabilities, see Materials and Methods) (Fig. 2B and 2C). However, in contrast to previous studies (*15–18*), flies rarely landed at or near the target. This discrepancy might reflect the fact that, different to these previous studies, our odorant delivery device was outside the wind tunnel. Positioning the odor delivery outside the wind tunnel prevents turbulences which could provide localization cues for the fly to land. Rather, our wind tunnel setting mimics better an odor source at distance.

When presenting the attractive odorant BN, depending on the experiment, 85 – 96 % of flies started flying (Table S1), and the average latency to flight was 10 – 21 s (Table S1, Fig. S1H, S1J and S2D, S2E), corresponding to approximately 5 to 10 odorant stimuli before taking off. For the aversive odorant BZ, 68 % of flies started flying, and average latency to flight was 27 s, corresponding to approximately 13 odorant stimuli before taking off. Similarly, as compared to the attractive odorant BN, fewer flies started flying when stimulated with the aversive odorant BA (68 – 84 %) or with a blank air control (Air) (71 %).

Attraction towards asynchronous mixtures of odorants with opposing innate valence

To test whether flies can detect stimulus onset asynchrony, we presented BN (A) and BA (B) either as single odorants, combined in a synchronous mixture (AB) or in asynchronous mixtures in which B preceded A by 33 ms (B33A) (Fig. 3A). Note that we used the odorant pair BN/BA to test the effect of stimulus onset asynchrony rather than BN/BZ because the differences in stimulus dynamics between BN and BZ makes this odorant pair unsuitable for generating synchronous mixtures (Fig. S1).

Flies showed a higher approach probability for the attractive odorant A compared to the aversive odorant B ($p(A > B) = 0.998$) or to the synchronous mixture AB ($p(A > AB) = 0.993$) (Fig. 3A). Moreover, flies showed a higher approach probability for the asynchronous mixture B33A compared to synchronous mixture AB ($p(B33A > AB) = 0.996$) or to the aversive odorant B ($p(B33A > B) \geq 0.999$). This shows that flies perceive the synchronous mixture AB and the asynchronous mixture B33A differently, with the onset asynchrony making the mixture more attractive.

To test whether flies are sensitive for shorter onset asynchronies we applied synchronous and asynchronous mixtures which started with B and with onset times differing by 5, 10 or 33 ms (B5A, B10A, B33A) (Fig. 3B). Flies presented with odorant A showed more activity in general, along with a higher visit probability near the target compared with flies presented with B. Flies showed a similar visit probability map for the synchronous mixture AB as for the aversive odorant B. However, when stimulated with the asynchronous mixtures B33A or B5A – but not B10A, flies showed more activity near the target compared to AB and B.

To make the quantification of flies' approach behavior more sensitive for the differences in odor valences and to account for the fact that flies distributed differently in the two different wind tunnels and experimental sets, we calculated an approach area that segregated flies' approach probabilities for the attractive odorant A and the aversive odorant B the most (Fig. 3C, Fig. S1-S3). We determined this area for each experimental set separately (see Materials and Methods). Note that this method maximizes the differences in approach probability between odorants A and B by design. Therefore, we refrain from comparing flies' approach probabilities for A or B and restrict the comparisons to the mixtures.

The flies' responses to the mixtures depended on the timing between B and A (Fig. 3D). For onset asynchronies of 5 ms (B5A) and 33 ms (B33A), flies were attracted to the target and scored a higher approach probability than for the synchronous mixture AB ($p(B5A > AB) = 0.984$, $p(B33A > AB) = 0.998$),

similar to that of A alone. However, for the onset asynchrony of 10 ms (B10A), flies' approach probability was not different to the approach probability for AB ($p(B10A > AB) = 0.783$). While this delay-specific approach probability is somewhat surprising, we acknowledge that the responses of third-order olfactory neurons (Kenyon cells) to asynchronous mixtures can also be delay-specific, which could account for this result (*19*).

Next, we wanted to discern whether the order in which odorants are presented in a mixture affects how a fly perceives the mixture. We used the same paradigm and odorants as before and stimulated flies with the synchronous mixture AB, the asynchronous mixture A33B (A precedes B) and B33A (B precedes A) (Fig. 3 E and S2). In this paradigm, flies showed a lower approach probability to the synchronous mixture AB than to the asynchronous mixture B33A ($p(B33A > AB) = 0.957$)), confirming our previous result that B33A is perceived differently to AB, and is perceived by the fly as more attractive. However, the approach probability for the asynchronous mixture A33B was not significantly different to the approach probability for AB ($p(A33B > AB) = 0.793$)), indicating that the two asynchronous mixtures A33B and B33A may have been also perceived differently.

These data show that flies can discriminate between the synchronous mixture AB and asynchronous mixtures B5A and B33A, supporting the hypothesis that flies can use stimulus onset asynchrony to segregate the attractive component A from the mixture of A and B even if they never encountered A alone (in B5A and B33A, B started before A and A ended at the same time as B). In contrast, the similar low approach probabilities for the aversive odorant B and the synchronous mixture AB is consistent with the hypothesis that flies perceive AB as coming from one source.

Attraction towards asynchronous mixtures of odorants with opposing learned valence

Finally, we wanted to determine whether flies' capability to discriminate between synchronous and asynchronous mixtures only works for odorants with opposing innate valence, or whether it also works for odorants with opposing learned valences. To address this question, we used an autonomous differential conditioning paradigm and paired one odorant (positively conditioned stimulus, CS+) with a 1M sucrose solution and another odorant (negatively conditioned stimulus, CS-) with a saturated NaCl solution (Fig. 3F). We used the odorants EA and BD equally often for CS+ and CS-. This procedure eliminates all non-associative effects of the conditioning procedure (e.g., sensitization), which would also change flies' responsiveness (*20*). Thus CS+ and CS- only differ with regards to the learned valences, devoid of innate, odorant-specific valences.

Also in this experiment, flies discriminated between synchronous and asynchronous mixtures, and showed lower approach probabilities to the synchronous mixture of the CS+ and the CS- (CS+CS-) than to the asynchronous mixture CS+33CS- or CS-33CS+ ($p(CS+33CS- > CS+CS-) = 0.965$, $p(CS-33CS+ > CS+CS-) = 0.981$) (Fig. 3G and S3). Together, these findings support the hypothesis that flies can use stimulus onset asynchrony to segregate odorants with both learned and innate valences from mixtures.

Discussion

We asked whether *Drosophila* can use stimulus onset asynchrony to segregate mixed odorants from different sources. We found that flies show stronger attraction to an asynchronous mixture of an attractive and an aversive odorant (mimicking two odorant sources) than to a synchronous mixture (mimicking one source). These results indicate that the fly's olfactory system uses stimulus onset asynchrony for olfactory object segregation, analogous to how humans' auditory and visual systems use stimulus onset asynchrony for concurrent sound segregation (*21*) and figure-ground segregation (*22*).

Odor-source segregation

Previous studies showed that animals perceive different odorants from the same source as one object while they perceive odorants from different sources as separate objects. In a pioneering study, Hopfield and

Gelperin (*7*) aversively conditioned slugs to the mixture of two food odors, A and B. When A and B were homogeneously mixed during conditioning (to mimic one odor source), slugs showed aversive responses to the homogenous mixture AB but not A and B alone. However, when A and B were heterogeneously mixed during conditioning (to mimic multiple sources), slugs also showed aversive responses to A and B alone. This suggests that slugs perceived the homogenous mixture AB as different from A or B, while they perceived the heterogeneous mixture as distinct odor objects A and B. Similarly, several arthropods species can segregate attractive from aversive odorants depending on whether both are released from the same source (forming a homogeneous mixture) or from different sources (forming a heterogeneous mixture) (*8–12*, *23*)).

In the above studies, animals could have achieved odor source segregation by detecting the heterogeneous distribution of odorants through a spatially heterogeneous activation across or within their olfactory organs, or they may have recognized the single odorants during bouts of their pure, unmixed presence. Compared to the above animals, *Drosophila* has tiny olfactory organs. Therefore, in lack of spatial resolution, *Drosophila* might use temporal rather than spatial stimulus cues for odor source segregation. Our data suggest that already 5 ms onset asynchrony is sufficient for *Drosophila* to segregate odorant sources, and this also works when the target is never encountered alone (in BΔtA, the target odorant A is always mixed with B, because A starts after and ends with B).

Mechanisms of odor source segregation

The odor-source segregation paradigms that were used in previous studies and in the present study were odor recognition tasks in which the odorants either had innate valences (*8*, *9*, *12*, *23*) or learned valences (*7*, *10*, *11*), and it is unknown whether animals can segregate mixtures of novel odorants that have no innate or learned valence. Thus, in previous studies and our own study, to recognize the odorants A and B, the olfactory system has to match the odor-evoked neural activity patterns to a neural template of A and B. The neural templates could have developed through evolution (e.g., odorants with innate valence activate specific, valence-encoding neurons in the lateral horn (*24–27*)), or by associative learning (odorants with learned valence activate specific, valence-encoding neurons in the mushroom body (*28–30*)).

Flies' capability to segregate two mixed odorants A and B based on a few milliseconds onset asynchrony poses temporal constraints on the neural code for odors. The computations that the olfactory system could use to perform odorant segregation are coupled to how the animal perceives the single odorants and their mixtures. As we do not know what the flies actually smell, but we can measure their attraction towards the odorants, we can only speculate about the perceptual differences between synchronous and asynchronous mixtures. In the following we shall discuss two alternative mechanisms of odor source-segregation based on temporal stimulus cues.

Shift from synthetic to analytic mixture processing?

Flies could perceive the synchronous mixture AB synthetically such that information about the components A and B is lost (AB ≠ A + B), while they perceive the asynchronous mixture AΔtB analytically such that information about A and B is preserved (AΔtB = A + B).

Behavioral experiments in honey bees provide support for synthetic processing of synchronous mixtures: when conditioned to an odorant mixture, bees show lower response probabilities for the individual components than for the conditioned mixture (*31*). Further evidence for synthetic mixture processing is provided by bees' capability to solve biconditional discrimination (*32*) and negative patterning tasks (*33*).

Physiological experiments also indicate that synchronous mixtures are processed synthetically, while asynchronous mixtures are processed more analytically. Mixing of multiple odorants changes the neuronal response patterns across olfactory receptor neurons and second-order olfactory neurons (projection neurons) such that component information gets partly lost (*19*, *34–37*). In contrast, the responses of projection neurons to asynchronous mixtures partly match those evoked by the individual components, with

the first arriving odorant often dominating the response pattern (*11*, *19*, *38*, *39*). However, such dominance of the first arriving odorant occurred neither in behavioral experiment in honey bees (*10*) nor in flies (this study). We therefore conclude that an asynchrony-induced shift from synthetic to a more analytic mixture representation cannot fully explain the behavioral odor source segregation observed in flies.

Analytical mixture processing and parallel encoding of source separation?

Alternatively, flies could perceive the identities and/or valences of both synchronously and asynchronously mixed odorants A and B analytically, and the information that odorant A and B belong to the same or to different sources could be directly encoded in the timing between A- and B-activated identity- or valence-encoding neurons.

Although there is evidence for synthetic processing of synchronous mixtures in insects (*31–33*), there is also evidence for analytical mixture processing: when honey bees are trained to respond to a multi-odorant mixture and afterwards are tested with the single odorants, they respond to most of the odorants (*40*, *41*). Analytic mixture processing has also been demonstrated in blocking experiments, in which previous conditioning to odorant A reduces (or blocks) conditioning to B during training with AB, because A already predicts the reward (*42*). Experiments in *Drosophila* provide further evidence for analytical mixture processing, as flies' responses to the synchronous mixture of two odorants with opposing valences A and B add up linearly (*43*, *44*). Moreover, *Drosophila* fails in biconditional discrimination or negative patterning tasks, which require synthetic mixture processing, suggesting that *Drosophila* processes mixtures analytically (*45*).

In accordance with these behavioral indications of analytic mixture perception, neuronal response properties would support analytical mixtures processing: even though mixtures suppress the response strength of olfactory neurons, those neurons that respond strongly to the components generally also respond strongly to the mixture (*11*, *19*, *34*, *35*, *39*). Thus, the across-neuron activity pattern evoked by the synchronous mixture largely includes the across-neuron activity pattern evoked by the single components. Moreover, *Drosophila* Kenyon cell responses to a mixture AB resemble the superposition of their responses to the single components A and B (*46*). Therefore, the neuronal representations of both synchronous and asynchronous mixtures likely contain sufficient odorant component information to allow for analytic mixture processing.

Whether or not two odorants A and B originate from one or two sources could be detected by coincidence-detecting neurons that receive input from valence-encoding neurons of the lateral horn (for odorants with innate valences; (*24–27*)) or from output neurons of the mushroom body (for odorants with learned valences; (*28–30*)). Those coincidence-detecting neurons would respond to synchronous input from the A- and B- activated valence-encoding neurons (A and B come from one source) but not to asynchronous input (A and B come from different sources). Coincidence detection could be mediated by NMDA glutamate receptors (*47*). The existence of glutamatergic neurons and NMDA receptors in both the lateral horn and in the mushroom body (*48*), and of glutamatergic valence-encoding mushroom body output neurons in *Drosophila* (*29*, *49*), is consistent with this hypothetical mechanism.

Detecting asynchronies of a few milliseconds between the neural representations of odorant A and B requires temporally precise encoding of odorant onsets – a requirement that appears to be fulfilled by insect olfactory receptor neurons (*50–52*). In particular, *Drosophila* olfactory receptor neurons respond to odorants rapidly (with first spike latencies down to 3 ms) and across neurons of the same type, the standard deviation of the first spike latencies can be as low as 0.2 ms (*53*). This high temporal precision of first odorant-evoked spikes across olfactory receptor neurons would allow a rapid, spike timing-based coding scheme for odorant onset and identity (*13*, *53*, *54*), which could underlie flies' capability to segregate odorants based on onset asynchrony.

Materials and Methods

Animals

Wild-type Canton S *Drosophila melanogaster* were reared on standard medium (100 mL contain 7.1 g cornmeal, 6.7 g fructose; 2.4 g dry yeast, 2.1 g sugar beet syrup, 0.7 g agar, 0.61 ml propionic acid, and 0.282 g ethyl paraben) under a 12:12 hours light:dark cycle (light from 09:00 to 21:00), at 25 °C and 60% relative humidity. All flies used in the experiments were female, aged between four and eight days old.

Wind tunnel

We carried out experiments in two wind tunnels, referred to here as wind tunnel 1 (WT 1, data shown in Fig. 3D) and wind tunnel 2 (WT 2 data shown in all other figures). We filmed each experiment using Raspberry Pi cameras (Raspberry Pi Camera Module v2; Raspberry Pi 3 model B) for 2 or 3 minutes with a resolution of 640 x 480 pixels and 90 frames s^{-1}; the first 10 seconds of flight duration was used for the analysis.

Both wind tunnels were constructed from clear Plexiglas. The inner side walls and floor were covered by a random checker board pattern (grey on white paper). The dimension of WT 1 was 1.2 m x 0.19 m x 0.19 m and of WT 2 was 2 m x 0.40 m x 0.40 m. The exhaust took in room air (28 °C, 60 % relative humidity) through the tunnel and removed it from the setup building via a ventilation shaft. An aluminum honeycomb grid (hole diameter x length: 0.53 cm x 3 cm, WT 1; 0.32 cm x 9.7 cm, WT 2) at the inlet and a grid at the outlet of the tunnel created a laminar flow throughout. The wind speed was 0.4 m s^{-1}. We injected odorants into the inlet of the wind tunnel with an olfactory stimulator (*14*). The outlet of the olfactory stimulator was 1 cm in diameter and was placed just outside of the honey comb grid, creating a laminar odorant plume within the tunnel. Flies entered the tunnel through a glass tube that was connected to a take-off platform whose center was 7.5 cm (WT 1) or 6 cm (WT 2) downstream from the inner side of the honeycomb grid. We also placed a black platform near the odor source, as recent studies have demonstrated that *Drosophila* stimulated by an attractive odorant approach dark spots (*17*, *18*). In WT 1 we used two cameras to film the flies. One camera was placed above the wind tunnel to capture the x-y plane of movement, whereas the other was placed at the side of the wind tunnel (90° to the other camera), thus capturing the movement of the fly within the z-y plane. The volume filmed measured 17.3 cm x 17.3 cm x 13.0 cm (x, y, z). In WT 2 we used a single camera placed above the wind tunnel to record the fly trajectories in the x-y plane. In order to capture the z-y plane of the flight track, we positioned a mirror at a 45° angle to the camera inside of the wind tunnel. The volume filmed measured 13.7 cm x 10.3 cm x 9.5 cm (x, y, z). Both wind tunnels were illuminated with indirect, homogeneous, white light with a color temperature of 6500 K (WT 1: compact fluorescent light, tageslichtlampe24.de; WT 2: LEDs, led-konzept.de). Additionally, we used 830 nm backlight illumination to get contrast-rich images of the flies.

Odorant delivery

We measured flies' odor tracking behavior using either odorants with innate (Fig.s 2 and 3) or conditioned (Fig. 3) valence. The pairs of odorants with innate valence used were 2-butanone (BN) and butanal (BA), and 2-butanone and benzaldehyde (BZ). For the conditioned odorants, we used 2,3-butanedione (BD) and ethyl acetate (EA). All odorants were supplied by Sigma Aldrich. We chose these odorants based on their valences measured in tethered flying flies (*44*). In this study, BN is innately attractive, whereas BA and BZ are innately aversive, and both BD and EA are slightly innately attractive. Throughout all experiments, innately attractive odorants were referred to as A and innately aversive odorants as B.

Odorants were delivered into the wind tunnels using a custom-made multichannel olfactory stimulator (*14*). Pure odorants were stored in 20 ml glass vials (Schmidlin) sealed with a Teflon septum. The cross section of the odorant surface was 3.1 cm^2. The headspace of odorized air was permanently drawn into the air dilution system using flowmeters (112-02GL, Analyt-MTC) and an electronic pressure control (35898;

Analyt-MTC). The stimulator had three channels: one for each odorant and one for blank air. The odorant vials were constantly flushed with clean air throughout the experiment, so that the headspace concentration reached a steady state of odorant evaporation into the air and odorant removal by the air flush. Note that due to the permanent air stream the headspace odorant concentration never saturated. The total flow per odorant channel was always 300 ml min^{-1}. In WT 1, BN was released at 50 ml min^{-1} and added to 250 ml min^{-1} air, and BA was released at 30 ml min^{-1} and added to 270 ml min^{-1} air (experiments in Fig. 3). In WT 2, BN, BA and BZ were released at 50 ml min^{-1} and were added to 250 ml min^{-1} air (experiments in Fig.s 2 and 3). For the conditioned odorants we used the PID to determine the head space concentrations in the conditioning tubes (see below) by moving the PID needle rapidly into the conditioning tubes to prevent dilution in odorant concentration due to air suction of the PID. These concentrations from the conditioning paradigm were then adjusted in the odor delivery device by measuring the odorant concentration just above the take-off platform with the PID. EA was released at 4 ml min^{-1} and added to 296 ml min^{-1} air, and BD was released at 1.84 ml min^{-1} and added to 298.16 ml min^{-1} air (experiments in Fig. 3).

The two odorant channels and a blank channel (each with an airstream of 300 ml min^{-1}) were combined and injected into a carrier air stream of 410 ml min^{-1} and, resulting in a total air flow at the outlet of the stimulator of 1.31 L min^{-1}, and a wind speed of 0.4 ms^{-1}.

Stimuli were presented either as single odorants (either A or B), as a synchronous mixture of odorants presented simultaneously (AB) or as an asynchronous mixture, with different time delays between the release of the odorants. In BΔtA, B starts before A, with Δt being either 5 ms, 10 ms and 33 ms. In AΔtB, A starts before B, with Δt being 33 ms (Fig. 1C). Note that the trailing odorant ended at the same time as the preceding odorant. Stimuli were delivered in odorant pulses of 500 ms, and the interstimulus interval was 2 s. To exclude that differences in flies' approach behavior towards the asynchronous and synchronous mixture reflected responses to mechanical cues produced by valve switching, we applied the single odorants together with a 33 ms delayed blank stimulus (both stimuli ended at the same time).

During experiments, all odorants were removed from the wind tunnel via an exhaust into the outside atmosphere. Between experiments using different odorants, the stimulator valves were flushed out over night to remove any residual odorant. Valves were controlled by compact RIO systems equipped with digital I/O modules Ni-9403 and odorant delivery was controlled by software written by Stefanie Neupert in LabVIEW 2011 SP1 (National Instruments).

Experimental protocol for odorants with innate valence

Day 1: Between 13:00 and 16:00, approximately 100 adult flies were removed from standard corn meal agar food and were subjected to food and water starvation for 24 hours in a cage (30×30×30 cm, BugDorm-1, BugDorm) that allowed them to move around freely, in a room with an approximate relative humidity of 60%, a temperature of 25 - 28 °C and 12 hour daylight cycle.

Day 2: Between 15:00 and 20:00, individual, flying female flies were removed from the cage and placed into a PVC tube through which they could walk freely to enter the wind tunnel and reach the take-off platform. Once the fly reached the take-off platform, odorant stimulation started. Each fly was stimulated repeatedly with the same odorant stimulus. During one experimental session an equal number of flies were stimulated with the different stimuli (as shown in each data panel) so that day-to-day variation would affect the behavior to all stimuli equally. The order of stimuli was alternated. After each experiment we removed and discarded the fly.

Each different experimental paradigm was made up of different sets, depending on the presence and location of the black landing platform. In the preliminary experiments assessing attraction to upwind flow (BN/BA/Air), there was only one set, with the landing platform placed centrally at the location of the odor source. For the preliminary experiments assessing attraction in the wind tunnel (BN/BZ), the first set placed the landing platform 1.5 cm to the right of the odor source, whereas the second set place the platform at the odor source directly. In the experiments to assess onset delays (BN/BA), there was only one set, where the

black platform was located 0.5 cm to the right of the odor source (x-y plane). For the experiments assessing odorant order (BN/BA), the first set contained no landing platform, whereas the second set contained the landing platform at the location of the odor source.

Differential conditioning

Day 1: Between 15:00 and 16:00, approximately 100 adult flies were removed from standard corn meal agar food and put into a cage (30×30×30 cm, BugDorm-1, BugDorm) that contained a differential conditioning apparatus (Fig. 3F). Flies could move around freely at an approximate relative humidity of 30%, a temperature of 25 - 28 °C and normal 12 hour daylight cycle for 24 h.

We trained flies in a differential conditioning paradigm to associate one odorant (positively conditioned stimulus, CS+) with 1 M sucrose solution as the positive reinforcer and to associate another odorant (negatively conditioned stimulus, CS-) with saturated NaCl solution as negative reinforcer (Fig. 3F). We used BD and EA as conditioned odorants. We balanced the experiments so that in half of the experiments we used BD as CS+ and EA as CS- and vice versa. CS+ and sucrose solution and CS- and NaCl solution were applied via two horizontally positioned plastic tubes (15 ml, 120 x 17 mm; Sarstedt). Each tube contained 10 ml of either sucrose or NaCl solution and were plugged with a cotton wool to avoid spillage. The frontal 2 cm of each tube remained empty. The odorant was delivered into this empty space via diffusion through a shortened head of a needle (1.2 x 40 mm, Sterican) which ended 1.5 cm inside the empty space of the tube. The needle was connected with a 20 ml glass vial (Schmidlin) that contained the pure odorant and was sealed with a Teflon septum. Thus, to reach the sucrose or NaCl solution, flies had to move through odorized air inside the plastic tube.

Day 2: Between 15:00 and 16:00, the conditioning apparatus was removed and flies were subjected to food and water starvation for the following 24 h in a room with an approximate relative humidity of 60%, a temperature of 25 - 28 °C and normal 12 hour daylight cycle.

Day 3: Flies were tested in the wind tunnel as described above in the section **Experimental protocol for odorants with innate valence** (Day 2). The conditioning experiments also had two sets, depending on the location of the black landing platform. In the first set, the black platform was located 1.5 cm to the right of the odor source (x-y plane) and in the second set, the black platform was at the location of the odor source.

Stimulus dynamics

To assess the dynamics and precision of the different stimuli, we used a photoionization detector (PID; miniPID model 200B; Aurora Scientific) to record the concentration change of pulses of each of the odorant pairs (BN and BA, BN and BZ, BD and EA) within the wind tunnel. Each pulse had a duration of 500 ms, and an interstimulus interval of 7 s to allow the odorant to clear from the odor delivery device and/or PID and to allow the PID signal to return to baseline before the following pulse was given. We gave a sequence of 100 pulses, alternating between odorant A and odorant B (7 s interval between A and B), thus 50 pulses of each odorant. For each odorant pulse, we calculated the onset time as the time it took to reach 5 % of the maximum PID signal, and the rise time as the time it took for the PID signal to reach from 5 % to 95 % of its maximum. We also calculated the difference in both the onset times and in the rise times between each of the 50 pairs of pulses (A – B).

Calculating the distance to the target

To calculate the Euclidean distance to the source, we obtained the x, y and z coordinates of the fly for the first 10 s of flight of the recording. If the fly did not take off from the entry platform, we calculated its closest point to the source on the platform.

For WT 1, we used two cameras which were calibrated within a two pixel scale of each other, thus we did not scale them any further. Both cameras were triggered simultaneously with a TTL pulse, however to ensure that they did not go out of sync, all videos were aligned by first frame of flight. We calculated the Euclidean distance of the fly to the target:

413 Euclidean distance = $\sqrt{(x - x_0)^2 + (y - y_0)^2 + (z - z_0)^2}$

414 Where x, y and z are the coordinates of the fly's location in a particular frame, and x0, y0 and z0 are the
415 coordinates of the target.

416 For WT 2, a single camera was used to film the fly trajectories in the x and y plane. In order to record the
417 movement in the z plane simultaneously, a mirror was placed at 45° to the x-y plane. Thus on the right half
418 of the video recordings, the x-y plane was recorded, and on the left half of the video, the mirrored z-y plane
419 was recorded. However, this led to shrinking of the image in the left half, approximately 1.3 times smaller
420 than the original objects on the right half. Therefore, we calculated the fly's distance to the target in WT 2
421 by:

422 Euclidean distance = $\sqrt{(x - x_0)^2 + (y - y_0)^2 + ((z - z_0) * 1.3)^2}$

423 Where x, y and z are the coordinates of the fly's location in a particular frame, and x0, y0 and z0 are the
424 coordinates of the target

425 **Quantifying approach with the "half-distance threshold"**

426 In order to measure approach behavior, we used the halfway distance between the frontal border of take-
427 off platform and the target to determine the circular approach area around the target. In WT 1, we used a
428 value of 117 pixels (3.2 cm) for the radius and in WT 2 a value of 71 pixels (2.7 cm).

429 **Quantifying approach with the "maximized A-B difference threshold"**

430 In order to make the analysis more sensitive for the difference between the approach probabilities for the
431 attractive and the aversive odorants A and B, we defined an approach area that segregated the flies' approach
432 probability for A (or CS+) and B (or CS-). To determine the radius of this area, we took the Euclidean
433 distance to target for each fly that was exposed to the attractive odorant A (or CS+) alone or the aversive
434 odorant B (or CS-) alone; those flies that encountered mixtures of odorants were not incorporated in this
435 process. The minimum distances were arranged in ascending order, and at each distance, we counted the
436 number of flies from treatment A and treatment B that were included within this threshold distance. Thus
437 for each of these distances, we calculated the difference in approach probabilities by:

438 Difference in approach probabilities = $\frac{A_{in}}{A_{in}+A_{out}} - \frac{B_{in}}{B_{in}+B_{out}}$

439 Where A_{in} represents the number of flies that were presented with odorant A and were included below the
440 threshold, A_{out} is the number of flies presented with A but excluded above the threshold. B_{in} and B_{out} were
441 the same measures for the flies that were presented with odorant B. We then plotted the thresholding index
442 against the vector of minimum distances, and fitted a curve using locally weighted scatterplot smoothing
443 (Fig. 3C and S1D, S1E, S2C, S2C, S3B and S3C). We took the distance that corresponded to the maximum
444 peak of the curve as the radius of the approach area, as this point indicates the greatest separation between
445 the two treatment groups. Since we used treatments A and B in defining the approach areas, we did not
446 include these flies in the statistical analyses.

447 **Approach probability**

448 In both WT 1 and WT 2 we filmed two angles of the flight area. Thus in each wind tunnel, there were two
449 separate areas of approach, one for each of the two cameras for WT 1, and one for each side of the video
450 screen for WT 2 (mirrored and original view). To calculate the approach probability, we gave each fly a
451 binary score. The coordinate of each fly in every frame was recorded and tested as to whether it fell within
452 the approach area boundaries. If a fly entered the approach area at any frame within 10 seconds after take-
453 off, the fly was given a score of 1; if not, was given a score of 0. This was done for each camera (WT 1) or
454 video side (WT 2), and then the results were combined so that only if a fly was in both areas of approach at

the same time point, would it be given a score of 1. Finally, we calculated the proportion of flies in each treatment that entered the approach area to get the approach probability.

Visit probability maps

We extracted the x-y coordinates of the fly during the first ten seconds of flight. We divided the recording image into 20 x 20 pixel bins to create two visit probability maps. Each bin was represented by a cell in the map. We then plotted each coordinate point onto the visit map, giving the cell a score of 1 if one or more points fell into the bin, or a 0 if no points fell into the bin. A matrix of zeros was generated for those flies that did not fly from the entry platform. We calculated the mean for each pixel bin across all of the flies in a treatment group.

Response latency

We selected the flies that started flying within 10 000 frames after entering the take-off platform (111 s, corresponding to approximately 50 odorant pulses). We defined the individual response latency for each fly as the time point of flight minus the time point of entry onto the take-off platform.

Statistical Analysis

All statistics were performed using Bayesian data analysis, based on (*55*). To compare the approach probabilities, we fitted a generalized linear model using the iteratively reweighted least squares method for fitting. We assumed a flat prior and set a binomial family due to the binary nature of the data:

$$p(y_i|p_i,n_i) \sim \text{Binom}(p_i,n_i)$$

where y_i is the number of successes for treatment i, p_i is the probability of success for observation i, and n_i is the number of trials for treatment i. We used the link function "logit", which is commonly used for binomial data, to transform the expected values of the outcome variable (probability ranging from 0 to 1) into the range of the linear predictor. We extracted the estimated model parameters for each treatment and then back-transformed the linear predictor to the scale of the outcome variable.

We simulated 100 000 values from the joint posterior distribution of the model parameters. To obtain the fitted value for each treatment, we derived the linear predictor by multiplying the model matrix with the corresponding set of model parameters for each set of simulated values, and then back-transformed the results. We extracted the 2.5 % and the 97.5 % quantiles, creating a 95 % credible interval.

To calculate the certainties that one treatment group had a significantly different approach probability to another group, we compared pairs of treatment groups individually. The proportion of simulations in which one treatment group was higher than that of the compared treatment group represents the posterior probability that the first treatment group has a higher approach probability than the second group. In the figures, we used stars for comparisons between the synchronous mixture AB and the asynchronous mixtures, and we used different letters for comparisons between all stimuli. If the posterior probability was greater than 0.95, we determined the approach probabilities as significantly different (* or different letters). If the posterior probability was greater than 0.99 or 0.999, we indicated their significance as ** and *** respectively (not indicated for comparisons between all stimuli, see text for exact posterior probabilities).

To compare the response latencies across treatment groups, we fitted a linear model using the synchronous mixture AB as the reference level. Similar to an ANOVA, this fits a linear regression to the dataset but using a categorical predictor variable instead of a continuous one. Here, treatment is the categorical variable, which has several indicator variables. AB was always used as the reference level, thus the other indicator variables were either A, B, A33B, and B33A, or A, B, B5A, B10A and B33A, depending on the experimental design. The former is demonstrated in the equation below:

$$\hat{y}_i = \beta_0 + \beta_1 I(g_i = 1) + \beta_2 I(g_i = 2) + \beta_3 I(g_i = 3) + \beta_4 I(g_i = 4) + \beta_5 I(g_i = 5)$$

$$y_i \sim Norm(\hat{y}_i, \sigma^2)$$

Where y_i is the i-th observation and each β value corresponds to the model coefficients for each treatment group g. The residual variance is σ^2. We simulated from the posterior distribution of the model parameters 100 000 times to obtain the group means and the 2.5 % and 97.5 % quantiles.

To determine whether one treatment group showed a significantly higher response latency compared to another group, we obtained the posterior distribution of the difference between the means of the two groups, by calculating the difference for each draw from the joint posterior distribution of the group means. We then calculated the proportion of draws from the joint posterior distribution for which the mean of the first group was higher than the second group. If the posterior probability was higher than 0.95, it was deemed significantly different (*). If the posterior probability was higher than 0.99 or 0.999, we indicated their significance as ** and *** respectively. For all data analysis, R version 3.5.0 ("Joy in Playing") were used (*56*).

References

1. Z. Kourtzi, C. E. Connor, Neural representations for object perception: structure, category, and adaptive coding. *Annu. Rev. Neurosci.* **34**, 45–67 (2011).
2. J. K. Bizley, Y. E. Cohen, The what, where and how of auditory-object perception. *Nat. Rev. Neurosci.* **14**, 693–707 (2013).
3. C. G. Galizia, Olfactory coding in the insect brain: Data and conjectures. *Eur. J. Neurosci.* **39**, 1784–1795 (2014).
4. N. Uchida, C. Poo, R. Haddad, Coding and Transformations in the Olfactory System. *Annu. Rev. Neurosci.* **37**, 363–385 (2014).
5. J. J. Hopfield, Olfactory computation and object perception. *Proc. Natl. Acad. Sci.* **88**, 6462–6466 (1991).
6. A. Celani, E. Villermaux, M. Vergassola, Odor landscapes in turbulent environments. *Phys. Rev. X*. **4**, 1–17 (2014).
7. J. F. Hopfield, A. Gelperin, Differential conditioning to a compound stimulus and its components in the terrestrial mollusc Limax maximus. *Behav. Neurosci.* **103**, 329–333 (1989).
8. T. C. Baker, H. Y. Fadamiro, A. A. Cosse, Moth uses fine tuning for odour resolution. *Nature*. **393**, 530–530 (1998).
9. M. N. Andersson, M. Binyameen, M. M. Sadek, F. Schlyter, Attraction Modulated by Spacing of Pheromone Components and Anti-attractants in a Bark Beetle and a Moth. *J. Chem. Ecol.* **37**, 899–911 (2011).
10. P. Szyszka, J. S. J. S. Stierle, S. Biergans, C. G. G. Galizia, The speed of smell: odor-object segregation within milliseconds. *PLoS One*. **7**, e36096 (2012).
11. D. Saha *et al.*, A spatiotemporal coding mechanism for background-invariant odor recognition. *Nat. Neurosci.* **16**, 1830–9 (2013).
12. M. Weissburg, L. Atkins, K. Berkenkamp, D. Mankin, Dine or dash? Turbulence inhibits blue crab navigation in attractive-aversive odor plumes by altering signal structure encoded by the olfactory pathway. *J. Exp. Biol.* **215**, 4175–82 (2012).
13. C. Martelli, J. R. Carlson, T. Emonet, Intensity invariant dynamics and odor-specific latencies in olfactory receptor neuron response. *J. Neurosci.* **33**, 6285–6297 (2013).
14. G. Raiser, C. G. G. Galizia, P. Szyszka, A High-Bandwidth Dual-Channel Olfactory Stimulator for Studying Temporal Sensitivity of Olfactory Processing. *Chem. Senses*. **42**, bjw114 (2016).

15. S. A. Budick, M. H. Dickinson, Free-flight responses of Drosophila melanogaster to attractive odors. *J. Exp. Biol.* **209**, 3001–3017 (2006).

16. B. Houot, V. Gigot, A. Robichon, J.-F. Ferveur, Free flight odor tracking in Drosophila: Effect of wing chemosensors, sex and pheromonal gene regulation. *Sci. Rep.* **7**, 40221 (2017).

17. N. Saxena, D. Natesan, S. P. Sane, Odor source localization in complex visual environments by fruit flies. *J. Exp. Biol.* **221**, jeb172023 (2018).

18. F. van Breugel, A. Huda, M. H. Dickinson, Drosophila have distinct activity-gated pathways that mediate attraction and aversion to CO2. *bioRxiv*, 227991 (2017).

19. B. M. Broome, V. Jayaraman, G. Laurent, Encoding and Decoding of Overlapping Odor Sequences. *Neuron*. **51**, 467–482 (2006).

20. T. Tully, Drosophila learning: Behavior and biochemistry. *Behav. Genet.* **14**, 527–557 (1984).

21. R. A. Rasch, Perception of Simultaneous Notes Such as in Polyphonic Music. *Acustica*. **40**, 21–33 (1978).

22. M. Usher, N. Donnelly, Visual synchrony affects binding and segmentation in perception. *Nature*. **394**, 179–182 (1998).

23. A. A. Nikonov, W. S. Leal, Peripheral coding of sex pheromone and a behavioral antagonist in the Japanese beetle, Popillia japonica. *J. Chem. Ecol.* **28**, 1075–89 (2002).

24. G. S. X. E. Jefferis *et al.*, Comprehensive Maps of Drosophila Higher Olfactory Centers: Spatially Segregated Fruit and Pheromone Representation. *Cell*. **128**, 1187–1203 (2007).

25. E. Roussel, J. Carcaud, M. Combe, M. Giurfa, J.-C. Sandoz, Olfactory Coding in the Honeybee Lateral Horn. *Curr. Biol.* **24**, 561–567 (2014).

26. A. Strutz *et al.*, Decoding odor quality and intensity in the Drosophila brain. *Elife*. **3**, e04147 (2014).

27. J. M. Jeanne, M. Fişek, R. I. Wilson, The Organization of Projections from Olfactory Glomeruli onto Higher-Order Neurons. *Neuron*. **98**, 1198–1213.e6 (2018).

28. M. F. Strube-Bloss, M. P. Nawrot, R. Menzel, Mushroom Body Output Neurons Encode Odor – Reward Associations. *J. Neurosci.* **31**, 3129–3140 (2011).

29. Y. Aso *et al.*, Mushroom body output neurons encode valence and guide memory-based action selection in Drosophila. *Elife*. **3**, e04580 (2014).

30. T. Hige, Y. Aso, M. N. Modi, G. M. Rubin, G. C. Turner, Heterosynaptic Plasticity Underlies Aversive Olfactory Learning in Drosophila. *Neuron*. **88**, 985–998 (2015).

31. B. H. Smith, Analysis of interaction in binary odorant mixtures. *Physiol. Behav.* **65**, 397–407 (1998).

32. S. Chandra, B. H. Smith, An analysis of synthetic processing of odor mixtures in the honeybee (Apis mellifera). *J. Exp. Biol.* **201**, 3113–21 (1998).

33. N. Deisig, H. Lachnit, M. Giurfa, F. Hellstern, Configural olfactory learning in honeybees: Negative and positive patterning discrimination. *Learn. Mem.* **8**, 70–78 (2001).

34. N. Deisig, M. Giurfa, H. Lachnit, J. C. Sandoz, Neural representation of olfactory mixtures in the honeybee antennal lobe. *Eur. J. Neurosci.* **24**, 1161–1174 (2006).

35. A. F. Silbering, C. G. Galizia, Processing of odor mixtures in the Drosophila antennal lobe reveals both global inhibition and glomerulus-specific interactions. *J. Neurosci.* **27**, 11966–77 (2007).

36. D. Münch, B. Schmeichel, A. F. Silbering, C. G. Galizia, Weaker ligands can dominate an odor blend due to syntopic interactions. *Chem. Senses*. **38**, 293–304 (2013).

37. D. Münch, C. G. Galizia, Take time: odor coding capacity across sensory neurons increases over time in Drosophila. *J. Comp. Physiol. A.* **203**, 959–972 (2017).

38. T. Nowotny, J. S. J. S. Stierle, C. G. G. Galizia, P. Szyszka, Data-driven honeybee antennal lobe model suggests how stimulus-onset asynchrony can aid odour segregation. *Brain Res.* **1536**, 119–34 (2013).

39. J. S. J. S. Stierle, C. Giovanni Galizia, P. Szyszka, C. G. Galizia, P. Szyszka, Millisecond Stimulus Onset-Asynchrony Enhances Information about Components in an Odor Mixture. *J. Neurosci.* **33**, 6060–6069 (2013).

40. D. Laloi, B. Roger, M. M. Blight, L. J. Wadhams, M. H. Pham-Delegue, Individual learning ability and complex odor recognition in the honey bee, Apis mellifera L. *J. Insect Behav.* **12**, 585–597 (1999).

41. J. Reinhard, M. Sinclair, M. V. Srinivasan, C. Claudianos, Honeybees Learn Odour Mixtures via a Selection of Key Odorants. *PLoS One*. **5**, e9110 (2010).

42. B. H. Smith, S. Cobey, The olfactory memory of the honeybee Apis mellifera. II. Blocking between odorants in binary mixtures. *J. Exp. Biol.* **195**, 91–108 (1994).

43. M. Thoma, B. S. Hansson, M. Knaden, Compound valence is conserved in binary odor mixtures in Drosophila melanogaster. *J. Exp. Biol.* **217**, 3645–3655 (2014).

44. L. Badel, K. Ohta, Y. Tsuchimoto, H. Kazama, Decoding of Context-Dependent Olfactory Behavior in Drosophila. *Neuron*. **91**, 155–167 (2016).

45. J. M. Young, J. Wessnitzer, J. D. Armstrong, B. Webb, Elemental and non-elemental olfactory learning in Drosophila. *Neurobiol. Learn. Mem.* **96**, 339–352 (2011).

46. R. A. A. Campbell *et al.*, Imaging a population code for odor identity in the Drosophila mushroom body. *J. Neurosci.* **33**, 10568–81 (2013).

47. M. L. Mayer, G. L. Westbrook, P. B. Guthrie, Voltage-dependent block by Mg2+of NMDA responses in spinal cord neurones. *Nature*. **309**, 261–263 (1984).

48. I. Sinakevitch, Y. Grau, N. J. Strausfeld, S. Birman, Dynamics of glutamatergic signaling in the mushroom body of young adult Drosophila. *Neural Dev.* **5**, 10 (2010).

49. D. Owald *et al.*, Activity of defined mushroom body output neurons underlies learned olfactory behavior in Drosophila. *Neuron*. **86**, 417–427 (2015).

50. K. Sato *et al.*, Insect olfactory receptors are heteromeric ligand-gated ion channels. *Nature*. **452**, 1002–1006 (2008).

51. J. Schuckel, S. Meisner, P. H. Torkkeli, A. S. French, Dynamic properties of Drosophila olfactory electroantennograms. *J. Comp. Physiol. A Neuroethol. Sensory, Neural, Behav. Physiol.* **194**, 483–489 (2008).

52. P. Szyszka, R. C. Gerkin, C. G. G. Galizia, B. H. B. H. Smith, High-speed odor transduction and pulse tracking by insect olfactory receptor neurons. *Proc. Natl. Acad. Sci. U. S. A.* **111**, 16925–30 (2014).

53. A. Egea-Weiss, A. Renner, C. J. Kleineidam, P. Szyszka, High Precision of Spike Timing across Olfactory Receptor Neurons Allows Rapid Odor Coding in Drosophila. *iScience*. **4**, 76–83 (2018).

54. S. Krofczik, R. Menzel, M. P. Nawrot, Rapid odor processing in the honeybee antennal lobe network. *Front. Comput. Neurosci.* **2**, 9 (2009).

55. F. Korner-Nievergelt *et al.*, *Bayesian data analysis in ecology using linear models with R, BUGS, and Stan* (Academic Press, 2015).

56. R Core Team, R: A Language and Environment for Statistical Computing. R Foundation for Statistical

Computing. *R Found. Stat. Comput. Vienna, Austria*. (2012), (available at http://www.r-project.org).

Acknowledgements: We thank Stefanie Neupert for advice on the statistics and comments on the manuscript, C. Giovanni Galiza, Thomas Nowotny and Mario Pannunzi for comments on the manuscript and Cansu Tafrali for help with the experiments. **Funding:** This project was funded by the Human Frontier Science Program (RGP0053/2015 to PS). **Author contributions:** PS conceptualized and designed the study. YMG and AS performed the data collection. TT wrote the video processing script and provided expertise on the analysis. YMG and AS performed the video processing. AS performed the statistical analysis. PS, YMG and AS wrote and edited the manuscript. PS supervised the study. **Competing interests:** The authors declare that they have no competing interests. **Data and materials availability:** All data is either supplied in this paper or in the Supplementary Materials, or can be requested directly from the authors.

Figures

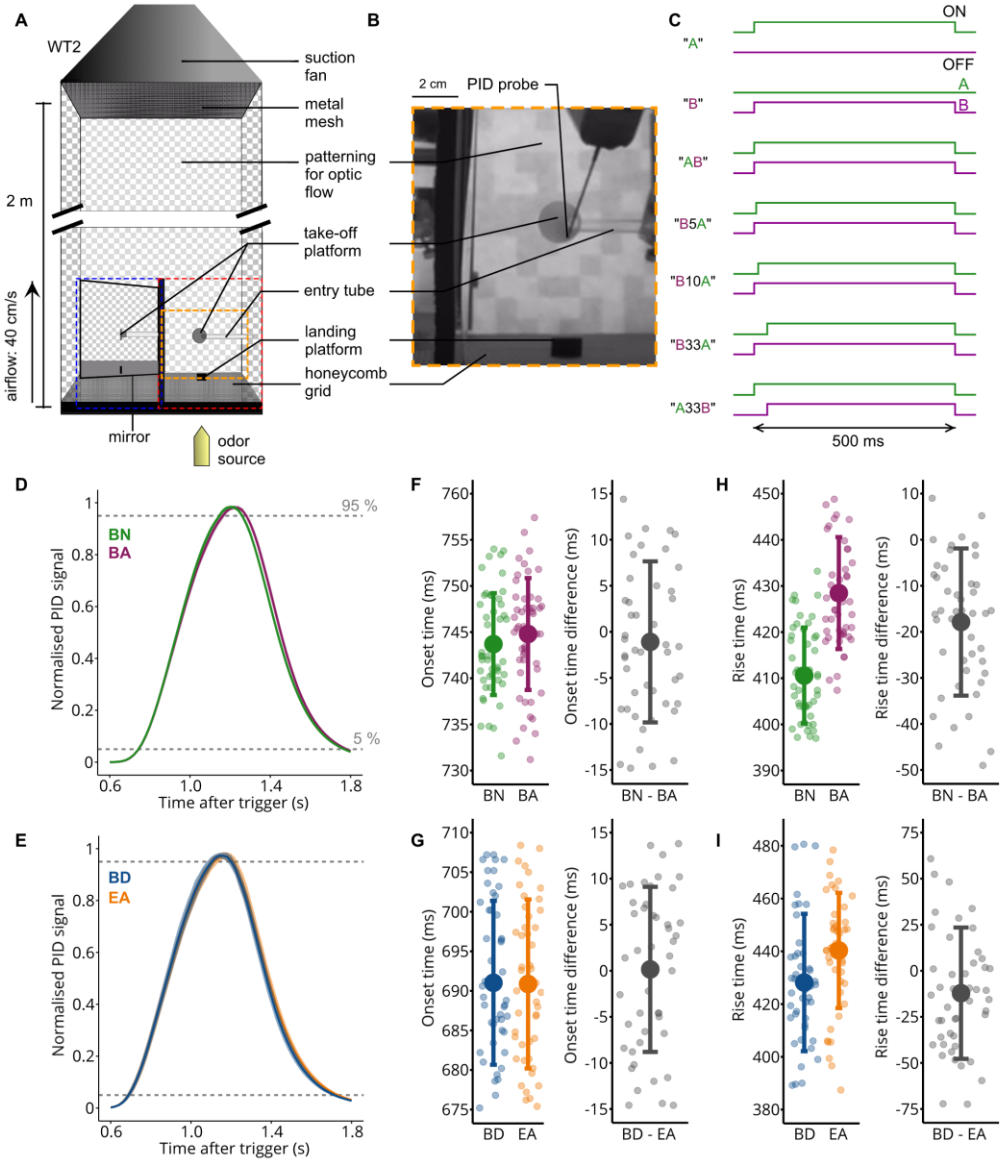

Fig. 1. Delivering temporally precise olfactory stimuli in a wind tunnel.

(**A**) Diagram of wind tunnel 2 (WT 2). Red and blue dashed boxes indicate the captured x-y and z-y planes respectively. The olfactory stimulator was placed outside of the wind tunnel to minimize turbulences. The orange box outlines in the diagram the image in (B). (**B**) The layout of WT 2, showing the position where the odorant concentrations were recorded using a PID. (**C**) Valve states for the different stimuli. The attractive odorant A and aversive odorant B are represented in green and magenta respectively. When asynchronous mixtures were presented, the first odorant was always given for 500 ms, and the following odorant with an onset delay. Both odorants had the same offset time. Pulses were repeated every 2 s. (**D**) PID recordings of pulsed stimuli for the odorant pair with innate valence 2-butanone (BN, green) and butanal (BA, magenta) (mean and SD over 50 pulses). Valves opened for 500 ms. Color code applies throughout the figures. Each PID signal was normalized to the maximum concentration reached. (**E**) Same as (D) for the odorant pair with conditioned valence 2,3-butanedione (BD, blue) and ethyl acetate (EA, orange), averaged over 50 pulses. (**F**) Left: Onset time (time taken to reach 5 % of maximum concentration

after valve trigger) for BN and BA (mean and SD over 50 pulses). Individual points represent the onsets for each pulse. Right: Onset time difference between pairs of BN and BA pulses (mean and SD over 50 pulses). (**G**) Same as (F) for BD and EA. (**H**) Left: Rise time (time take to reach 95 % of maximum concentration from the 5% onset time) for BN and BA (mean and SD over 50 pulses). Individual points represent the rise times for each pulse. Right: Mean rise time difference between pairs of BN and BA pulses (mean and SD over 50 Pulses). (**I**) Same as (H) for BD and EA.

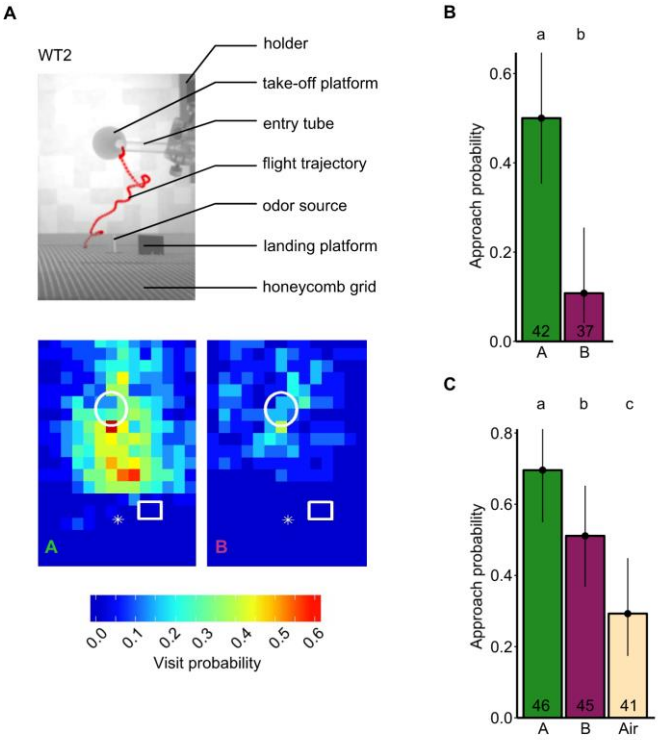

Fig. 2. Odor tracking in the wind tunnel.

(**A**) Top: Minimum intensity projection of a movie of a flying fly (red) in the wind tunnel during stimulation with A (BN). Bottom: Visit probability plot equivalent to top image for A (BN) and B (BZ) respectively in odorant pair BN/BZ (set 1). Each bin represents 20 x 20 pixels in the image, corresponding to 7.6 x 7.6 mm at the height of the landing platform. Each bin shows the mean binary value across flies. The take-off platform (white circle), landing platform (white rectangle) and odor source (white star) are indicated for position reference. n = 24 and 20 for A and B respectively. (**B**) Approach probability to cross the half distance between take-off platform and landing platform for BN (A) and BZ (B). Filled points represent the fitted value from the GLM. Error bars represent the 95 % credible intervals. The lower case letters represent significantly different responses for the different odorants; this applies throughout the figure. Numbers in bars indicate the number of flies; this applies throughout all figures. (**C**) Same as in B but for BN (A), BA (B) and a blank air stimulus (Air).

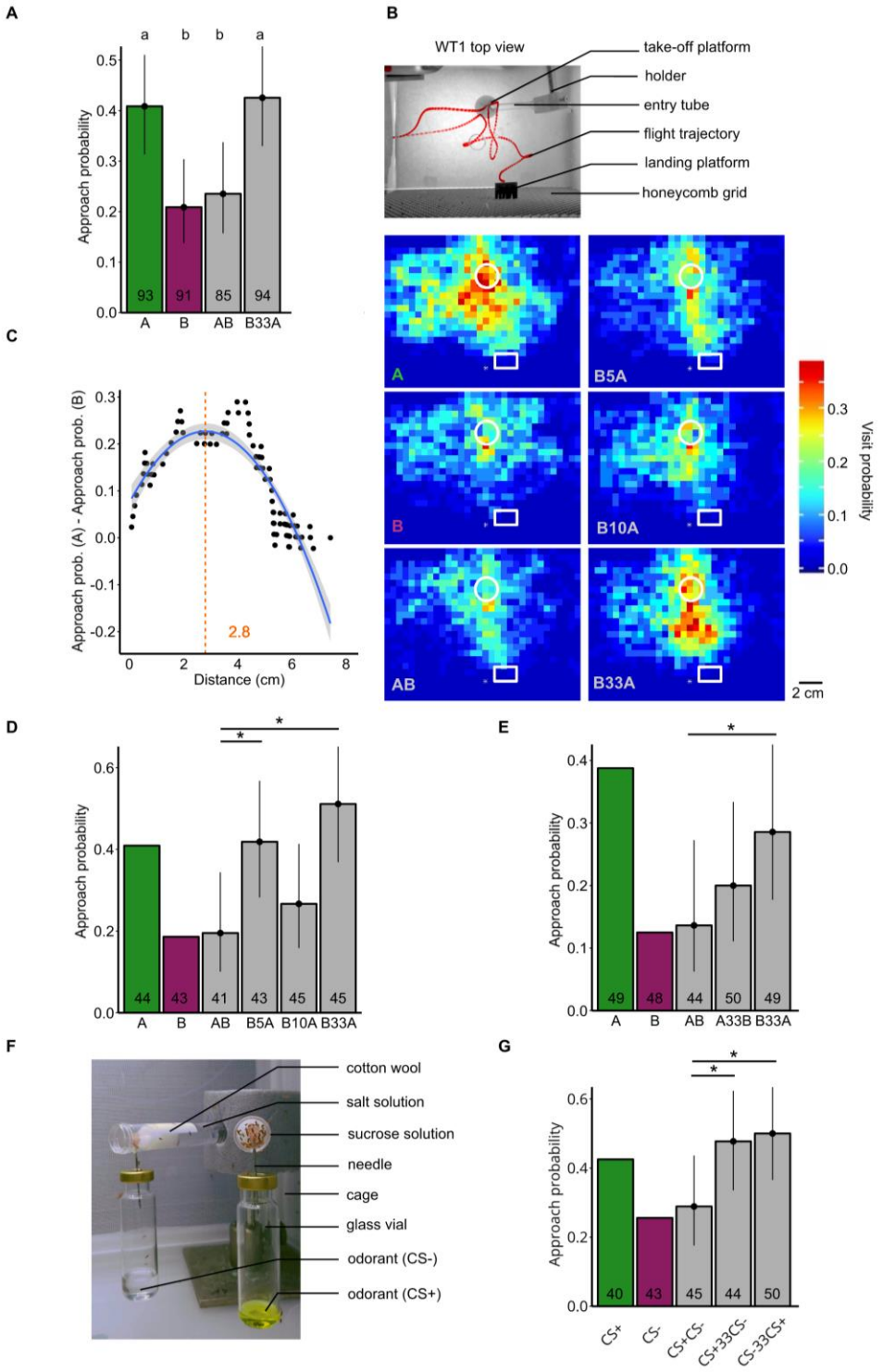

Fig. 3. Stimulus onset asynchrony makes a mixture of odorants with opposing innate or conditioned valence attractive.

(**A**) Approach probability determined by the half distance-threshold for the single odorants BN (A), BA (B), their synchronous mixture (AB) and their asynchronous mixture (B33A). Filled points represent the fitted value from the GLM. Error bars represent the 95 % credible intervals. The lower case letters represent

significantly different responses to the odorant treatments; this is the case throughout the figure (this dataset is pooled from experiments shown in (D) and (E)). (**B**) Top: Minimum intensity projection of a movie of a flying fly (red) in the wind tunnel during stimulation with BN (A). Bottom: Visit probability maps of the wind tunnel image in top for A (BN) and B (BA) and the synchronous (AB) and asynchronous (B5A, B10A, B33A) mixtures. The take-off platform (white circle), landing platform (white rectangle) and odor source (white star) are indicated for position reference. n = 44, 43, 41, 43, 45 and 45 for A, B, AB, B5A, B10A and B33A respectively. (**C**) Thresholding method that uses the distance which separates flies' approach probabilities for A and B best (see "maximized A-B difference threshold" in Materials and Methods). Each point represents the proportion of A-stimulated flies that approached the target by the given minimum distance minus the proportion of B-stimulated flies. The blue trend line was fitted using locally weighted scatterplot smoothing. The orange dashed line and value represents the peak of the trend line in cm. (**D**) Approach probability for odorant mixtures with different asynchronies, determined by the maximized A-B difference thresholding method shown in (C). Stars represent significantly different responses between AB and the other mixtures. Since A and B are used to determine the threshold, they were not included in the statistical analysis and thus do not have fitted values or credible intervals. (**E**) Approach probability for odorant mixtures presented using different odorant orders, using the maximized A-B difference thresholding method. (**F**) Image of the conditioning setup in which flies were left for autonomous differential conditioning. Flies can freely fly in the cage and enter the odorized tubes containing cotton wool soaked either with aversive salt solution or attractive sucrose solution. (**G**) Approach probability for odorant mixtures with conditioned valences, using the maximized A-B difference thresholding method. Odorants BD and EA were used equally as often as the CS+ and CS-. Points and error bars are the same in (A).